

Investigating the Kinetic Effects on Current Gradient-Driven Instabilities of Electron Current Layers via Particle-in-Cell Simulations

Sushmita Mishra¹, Gurudatt Gaur², Bhavesh G. Patel³

¹Institute of Advanced Research, Gandhinagar 382 426, India

²St. Xavier's College (Autonomous), Navrangpura, Ahmedabad 380 009, India

³Institute for Plasma Research, Bhat, Gandhinagar 382 428, India

E-mail: gurudatt.gaur@sxca.edu.in

E-mail: mishra.sushmita0@gmail.com

7 November 2024

Abstract. Electron current layers, which form in various natural and laboratory plasmas, are susceptible to multiple instabilities, with tearing being a prominent instability driven by current gradients. Tearing is considered a potential mechanism for magnetic reconnection in collisionless regimes, where electron inertia acts as a non-ideal factor that causes magnetic field lines to break and reconnect. In contrast, another mode, known as the surface-preserving mode, also driven by current gradients, maintains the magnetic field topology. In this study, we investigate the kinetic effects on these modes in the presence of finite electron temperatures using two-dimensional particle-in-cell simulations. Our findings reveal that temperature significantly stabilizes the tearing mode, particularly at higher temperatures, due to an increased electron Larmor radius and the associated magnetic field diffusion. We also examine the interplay between the guide field and temperature. Additionally, we observe that growth rates for the surface-preserving mode, in contrast to the tearing mode, increase with temperature, likely due to enhanced electron flow velocities. Furthermore, we identify cases with mixed modes, where both tearing and surface-preserving modes coexist, exhibiting asymmetric structures characteristic of asymmetric magnetic reconnection. Finally, we outline potential future research directions that build upon our findings.

1. Introduction

Plasma is a state of matter in which electrons and ions move, exhibiting collective behavior under the influence of electric and magnetic fields generated either by their own motion or by external sources. Magnetic fields significantly influence plasma dynamics, leading to rich and complex behaviors. They affect the motion of charged particles, which, in turn, modify the magnetic fields due to the “frozen-in” condition arising from plasma’s high electrical conductivity. A key phenomenon where the magnetic field is

altered by plasma particles is magnetic reconnection (MR). In MR, plasma pushes two oppositely directed magnetic field lines towards each other, changing the topology of the magnetic field lines [1, 2]. MR occurs in various natural settings, including within the solar system [3]. It plays a crucial role in solar flares, coronal mass ejections, the Earth's magnetosphere, and astrophysical jets, and is also believed to occur during star formation. Additionally, MR is observed in several fusion plasma devices, such as Tokamak, Reverse Field Pinch, and Spheromak configurations [4, 5]. Numerous laboratory plasma devices have been developed to investigate the mechanisms behind MR [6, 7, 8].

Significant efforts have been made to propose theoretical models that explain MR at different time and length scales in various plasma conditions. The resistive MHD (magnetohydrodynamics) models, such as the Sweet-Parker and Petschek models, describe MR occurring in long, narrow current sheets with a reconnection rate limited by plasma resistivity. The Sweet-Parker model [9, 10] predicts a slow reconnection rate, insufficient to explain the fast reconnection events observed in nature. In contrast, the Petschek model [11] suggests a faster reconnection process, although it is less applicable to collisionless plasmas. In space and astrophysics contexts, where fast reconnection occurs, plasmas are known to be collisionless. In a collisionless plasma, where the mean free path of particles is much larger than the system size, reconnection dynamics are predominantly governed by electromagnetic forces rather than collisional interactions.

Various models have been proposed to understand fast reconnection in collisionless plasmas, addressing different aspects and scales of the process, both fluid and kinetic. While the MHD model is valuable for understanding large-scale plasma behavior, it is insufficient for describing the detailed physics of collisionless MR. For collisionless plasmas, models that include electron-scale dynamics, such as EMHD (electron magnetohydrodynamics) [12, 13], Hall MHD [1, 3], and two-fluid models [14, 15, 2], as well as models that incorporate kinetic effects, such as hybrid [16] and full kinetic (PIC: particle-in-cell) models [17, 18], are necessary to accurately capture the complex dynamics and fast reconnection rates observed in these environments. These models incorporate the Hall term and electron inertia, leading to faster reconnection rates and more complex magnetic island structures than single-fluid MHD models can provide.

A specific manifestation of magnetic reconnection (MR) is the tearing instability, a dynamic approach to studying MR. Unlike steady-state approaches exemplified by the Sweet-Parker and Petschek models, the tearing instability involves the formation of a chain of magnetic islands and reconnection layers, leading to a reconfiguration of the magnetic topology. The tearing mode evolves according to parameters such as the width of the current sheet (ϵ) and length scales characteristic of kinetic effects, including the electron inertial skin depth (d_e), ion inertial skin depth (d_i), and Larmor radius of electrons or ions (r_L) [2]. The tearing instability in thin current layers with thickness smaller than the ion skin depth has been widely studied in the context of 2D and 3D EMHD.

Gaur and Kaw [13] investigated the susceptibility of thin electron current sheets to

tearing and surface-preserving instabilities within 2D EMHD when equilibrium length scales are shorter than the ion skin depth. These instabilities, driven by current gradients, exhibit distinct behaviors: the tearing mode results in magnetic island formation, while the surface-preserving mode maintains magnetic flux surfaces. The tearing mode is non-local, unstable to larger-scale perturbations, while the surface-preserving mode is local, unstable to shorter wavelength perturbations. Similar studies by Lukin [19] and Jain et al. [20, 21] have examined these modes within the EMHD framework.

Building on Gaur and Kaw’s work, we explore the kinetic effects on tearing and surface-preserving modes, specifically the influence of temperature and the interplay between temperature and guide fields, using 2D PIC simulations. To our knowledge, this is the first study to address these modes within a kinetic framework.

Fluid descriptions such as EMHD are inadequate at kinetic scales, particularly for high-temperature plasmas or when length scales approach the particle gyroradius. In situations dominated by high-frequency phenomena, strong magnetic fields, turbulence, or collisionless dynamics, a kinetic approach is necessary. PIC simulations, which treat particles individually rather than collectively as a fluid, allow us to capture the intricate kinetic behavior of plasmas [22]. In this study, we utilize PIC simulations to examine the linear and nonlinear evolution of tearing and surface-preserving instabilities in response to kinetic effects.

This paper is organized as follows. In Section II, we discuss the basics of the particle-in-cell scheme along with the simulation setup used to model tearing and surface-preserving instabilities in electron current layers (representing a thin electron current sheet). In Section III, we present and analyze the results from various simulation runs, focusing on the behavior of the tearing and surface-preserving modes in the presence of temperature. This section also includes a comparison with existing studies to highlight the novelty of our work. In Section IV, we provide conclusions and discuss future prospects of our research.

2. Particle-in-cell (PIC) method and Simulation Setup

Particle simulation model can be classified into three principal types: the particle-particle (PP) model, the particle-mesh (PM) model, and the particle-particle-particle-mesh (PPPM or P3M) model [23]. The PP model utilizes the action-at-a-distance approach of the force law, the PM model implements the force as a field quantity (approximating it on a mesh), and the P3M model incorporates characteristics of both the PP and PM models.

The Particle-in-Cell (PIC) method is based on the PM model. In PIC simulations, the plasma is represented by a large number of superparticles, each representing a cluster of real particles, typically electrons and ions. These superparticles move through a computational grid (mesh) where the electromagnetic fields are calculated. The position and velocity of each particle are given as initial conditions, which determine

the continuous distribution of the particles' position and velocity in space.

The PIC algorithm involves a self-consistent cycle: assigning charge to the mesh, solving Maxwell's equations and computing the fields from the mesh-defined potential, and updating the particle velocity and position based on the fields. Fig. 1 shows the algorithm for the PIC technique, which includes the Boris scheme for pushing particles and a finite difference solver for the field calculations. Various PIC codes are available for plasma simulations, with OSIRIS being one of the most widely used.

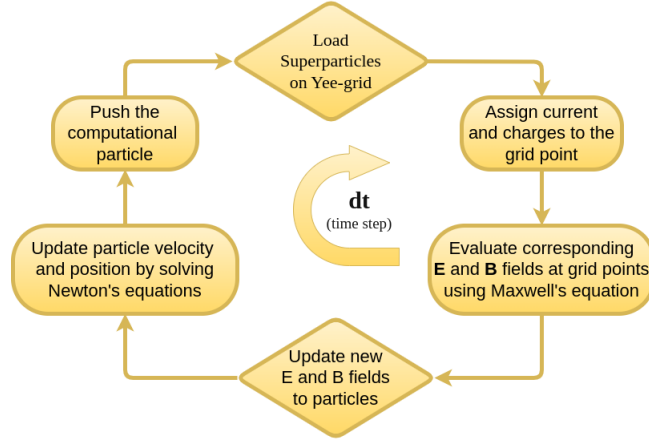


Figure 1. Overview of the PIC Algorithm Workflow

OSIRIS is a state-of-the-art PIC simulation code that is fully relativistic, massively parallel and fully object-oriented. Written in Fortran-90, it is designed for high-performance computing with multi-dimensional capabilities [24]. OSIRIS simulates the behavior of plasmas by solving the Vlasov-Maxwell equations using the PIC method and is optimized for large-scale parallel supercomputers, utilizing the Message Passing Interface (MPI) for communication between processors [25].

Widely used in plasma physics research, OSIRIS features comprehensive physics models, including electromagnetic fields, relativistic particle dynamics, collisions, and radiation mechanisms. It excels in modeling complex plasma interactions, such as laser-plasma interactions for inertial confinement fusion [26] and particle acceleration in astrophysical phenomena like magnetic reconnection, gamma-ray bursts, and relativistic jets [27].

We have utilized the OSIRIS 4.0 framework [28] to model the 2D tearing and surface preserving instabilities. In our simulations, the normalized units are defined as follows: length is normalized by electron skin depth c/ω_{pe} , time is normalized by ω_{pe}^{-1} , and magnetic field by the quantity $\frac{m_e c^2}{e(c/\omega_{pe})}$. Where c is the speed of light, ω_{pe} is the electron plasma frequency, and m_e is the electron mass.

We have initialized our simulations for a thin current sheet equilibrium having width of the magnitude ϵ and z is the symmetry direction i.e., $(\frac{\partial}{\partial z}) = 0$. Ions are at rest (i.e., $v_i = 0$). Equilibrium magnetic field is expressed as follows:

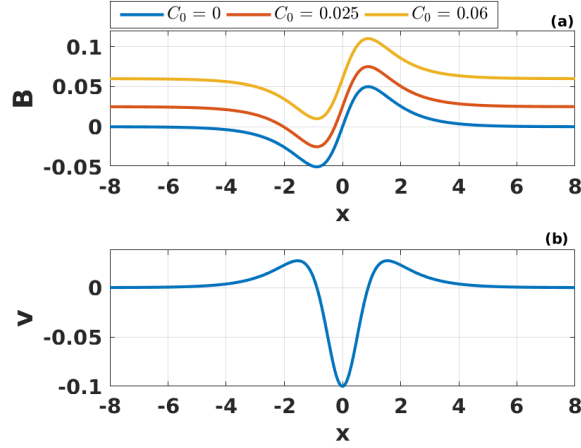


Figure 2. (a) Equilibrium magnetic field and (b) equilibrium velocity profiles.

$$\mathbf{B}_{eq} = \hat{y}B_0(x) = \hat{y}(B_{00}\{sech(x/\epsilon)\tanh(x/\epsilon)\} + C_0), \quad (1)$$

Corresponding equilibrium velocity is written as,

$$\begin{aligned} \mathbf{v}_{eq} \left(= -\frac{\nabla \times \mathbf{B}_{eq}}{n_0 e} \right) &= \hat{z}v_0(x) \\ &= \hat{z} \frac{B_{00} \sinh^2(x/\epsilon)}{(n_0 e) \epsilon \cosh^3(x/\epsilon)} \end{aligned} \quad (2)$$

Where, ϵ is shear width, B_{00} is the amplitude of the magnetic field, C_0 is a uniform magnetic field added externally in the direction of field.

In all our simulation runs, we have chosen $B_{00} = 0.1$ and $\epsilon = 1$. A 2D rectangular simulation box with dimensions $L_x = 8(c/\omega_{pe})$ and $L_y = 3(c/\omega_{pe})$ has been chosen. The spatial resolution corresponds to a grid size of $\Delta x = 2L_x/512$ and $\Delta y = 2L_y/256$. A uniform plasma number density $n_0 = 10^{18}cm^{-3}$ has been chosen. We allow the equilibrium to evolve against the numerical perturbations. We have taken a periodic boundary conditions for both fields and particles because the equilibrium profile chosen is such that it ceases at both the boundaries. The equilibrium magnetic field and the corresponding equilibrium velocity profiles are shown in Fig. 2. Three different magnetic field profiles corresponds to three different values of C_0 viz., 0, 0.025, 0.06.

3. Results and Discussion

In this section we present and discuss the results from various simulation runs obtained by varying the C_0 (a uniform magnetic field applied along the equilibrium magnetic field) and T (temperature).

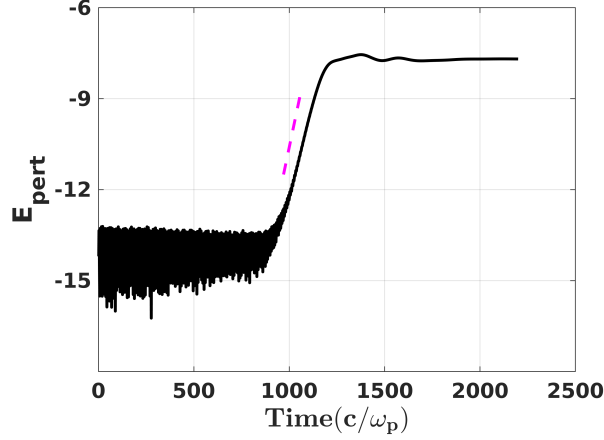


Figure 3. Evolution of perturbed energy over time. The dashed straight lines drawn alongside has a slope of 2γ , where $\gamma = 0.0188$ is the linear growth rate obtained from the linear analysis.

3.1. $C_0 = 0$: Only Tearing Mode Case

We begin by setting $T = 0$, corresponding to the typical tearing instability case, which has been extensively studied by various authors using both fluid and PIC simulations. We reproduced this scenario to validate our simulation setup. In Fig. 3, we plot the evolution of the perturbation energy over time. During the initial phase of the simulation, the perturbation energy grows exponentially. The slope of this portion (a straight line on the semilog plot) closely matches twice the maximum growth rate 2γ derived from linear instability calculations [13]. The dashed line alongside the simulation curve has a slope equal to 2γ , showing good agreement. As the amplitude of the perturbed field increases, nonlinear effects become significant, leading to the saturation of the perturbation energy in the later stages of the simulation.

In Fig. 4, the contours in the background depict the structure of the out-of-plane magnetic field. The magnetic field lines, superimposed on these contours, are straight, initially. However, as the tearing instability progresses, these field lines begin to bend, eventually forming an island structure. Concurrently, the out-of-plane magnetic field develops a distinctive quadrupolar pattern. These features are characteristic indicators of the tearing instability.

Having validated the simulation setup, we now proceed to study the effect of temperature on tearing instability. We conduct simulation runs for the following temperature values: ($T = 5, 10, 20, 50, 100, 200, 500, 1000$) electron volts. Upon increasing the temperature, while the characteristic features of the instability (such as the formation of islands and quadrupoles) remain more or less the same, we observe a variation in the growth rate with temperature. Fig. 5 illustrates the variation in the growth rate as temperature increases. The growth rate initially increases with temperature and then starts decreasing monotonically. This behavior can be understood as follows.

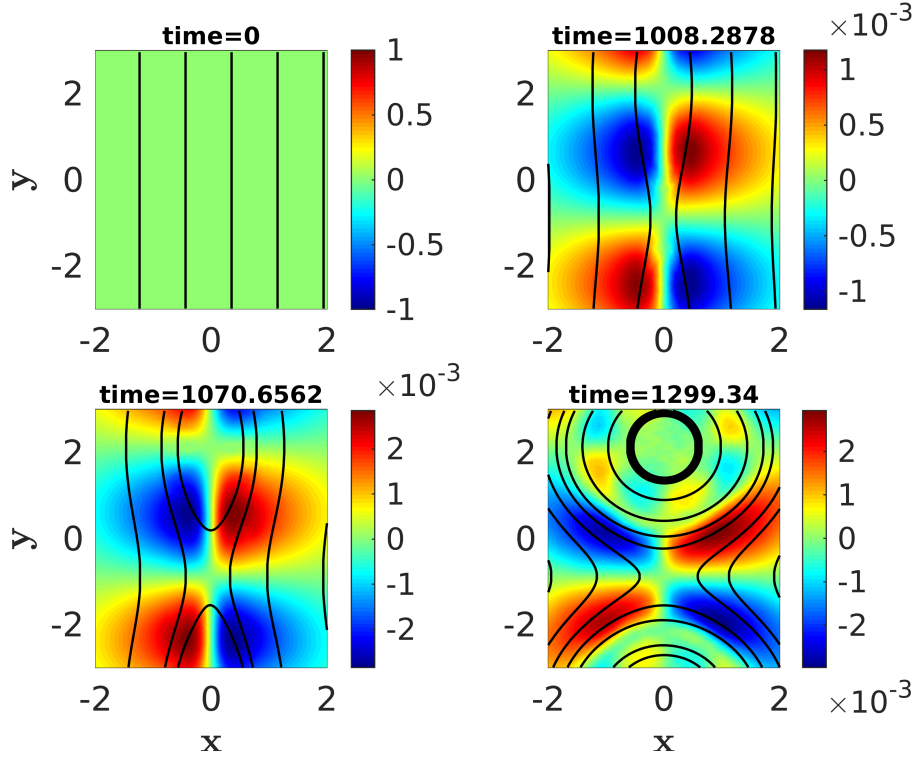


Figure 4. Shaded isocontours of out-of-plane magnetic field with superimposed streamlines (solid lines) over various times for pure tearing mode case ($C_0 = 0$) and $T = 0$ eV case.

Initially, when the temperature increases (say, up to 10 eV), the kinetic energy of the electrons increases. This makes the tearing instability more favorable, as the electrons move faster in the tearing instability plane compared to the case with $T = 0$. Consequently, the instability growth rate increases marginally. If the temperature further increases (beyond 10 eV), electron larmor radius (r_L) increases significantly, which is given as $r_L = v_{th}/\omega_{ce}$, where $v_{th} = \sqrt{p_e/(nm)}$ and $\omega_{ce} = eB/(m_e c)$ are the thermal velocity and plasma cyclotron frequency respectively. In other words, kinetic pressure starts dominating the the magnetic pressure i.e., the plasma beta (β) value increases, where $\beta = (n_e k_B T / (B^2 / 2\mu_0))$. This increases the diffusion of magnetic field (not just near the null-line) which, in turn, reduces the strength of current-gradient (due to weaker magnetic field and hence weaker current). As a result, the growth rate decreases. Eventually, at $T \geq 1keV$, the instability completely suppresses.

To reinforce our argument on the role of larmor radius in tearing growth rate against temperature, we add a uniform guide field \ddagger (in the direction perpendicular to the plane of tearing mode). Addition of guide field increases the magnetic pressure (energy) of the system. Owing to which, the decrease in the growth rate now start dropping at a higher temperature. Fig. 6 shows that as the guide field increases, the peak in the growth rate shift towards higher temperature.

\ddagger Presence of a guide field is known to play a stabilizing role in magnetic reconnection.

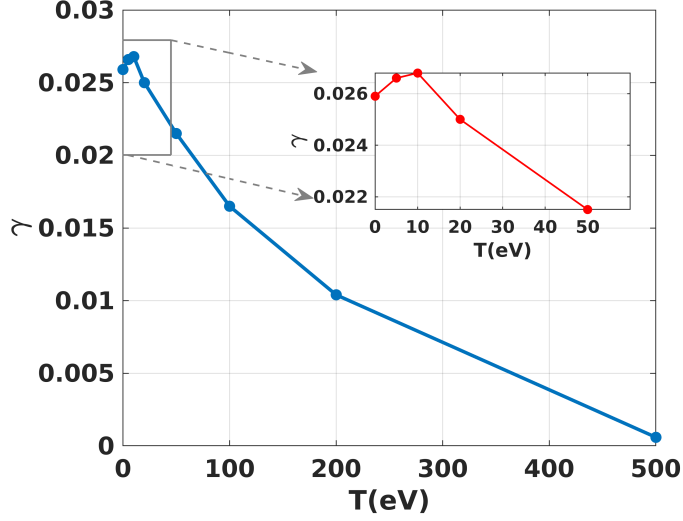


Figure 5. Variation in growth rate as a function of temperature (T) in eV, calculated from the perturbed energy evolution for the pure tearing mode case ($C_0 = 0$). The inset presents a closer look at the growth rates for temperatures of 0, 5, 10, 20, and 50 eV.

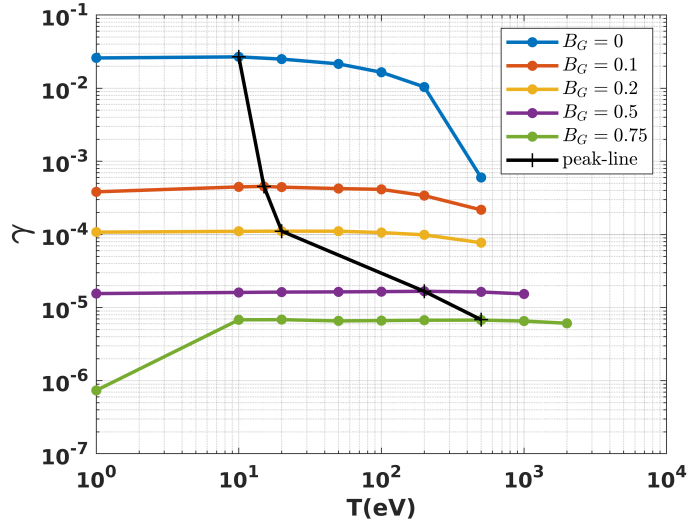


Figure 6. Growth rate of perturbed energy evolution for the pure tearing mode case ($C_0 = 0$) with different guide field values and varying temperatures. The black line denotes the peak value of each growth rate curve for the different guide field values.

3.2. $C_0 = 0.06$: Only Surface Preserving Mode Case

We now add C_0 , a uniform magnetic field along the direction of equilibrium magnetic field. We choose $C_0 = 0.06$, as this would make the condition $B_0 - B_0'' \leq 0$ for the existence of the tearing mode to be violated. Coincidentally, the opposite condition $B_0 - B_0'' > 0$ favors the existence of the surface preserving instability. Hence, only the surface preserving mode will be present in this case [13].

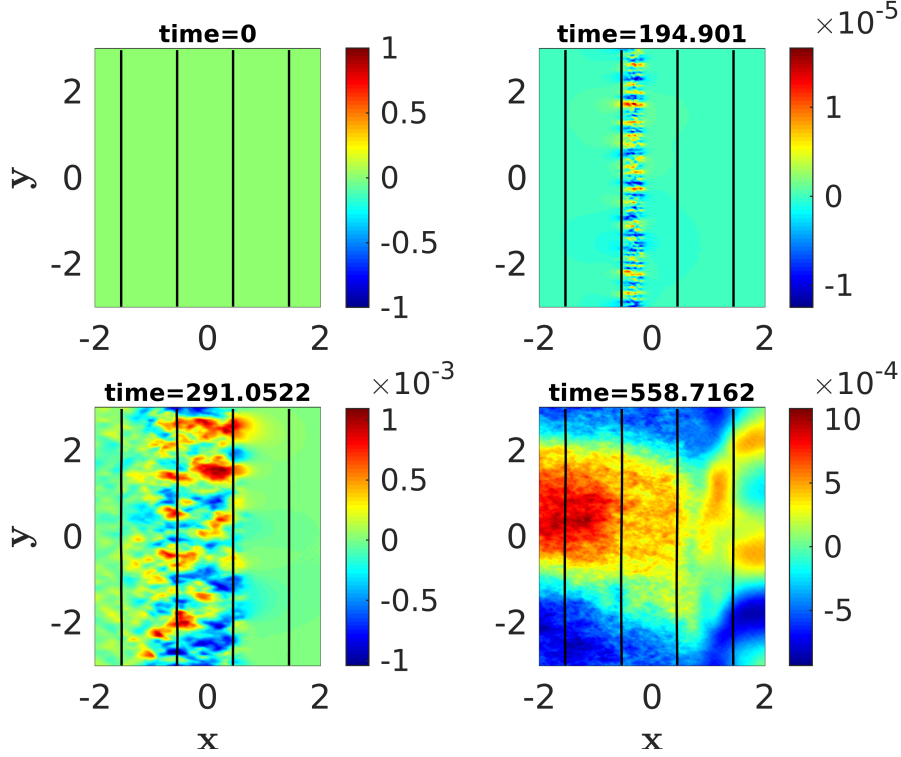


Figure 7. Shaded isocontours of out-of-plane magnetic field with superimposed streamlines (solid lines) over various times for the only surface preserving mode case ($C_0 = 0.06$) and $T = 0$ eV case.

Simulation run with $T = 0$ eV, show no formation of quadrupoles or islands, which is unlike the tearing mode scenario. Magnetic field lines in this case do not bend and instead form a channel-like structure, as depicted in Fig. 7. In order to understand the behaviour of growth rate of surface preserving mode we conduct simulation runs for the following temperature values: ($T = 5, 10, 20, 50, 100, 200, 500$) electron volts. In Fig. 8, we plot the growth rate vs temperature. In this case, the growth rate goes on to increase, unlike the tearing mode case where the growth rate first increases and then start decreasing after a certain temperature. This can be explained as follows. Surface preserving mode, also termed as stationary nontearing inertial scale mode, is driven by the electron flow perturbations along the direction of the current gradient[19]. An increase in temperature increases the electron flow velocity which, in turn, makes the instability more favourable.

3.3. $C_0 = 0.025$: Mixed Modes Case

In this last case, we choose $C_0 = 0.025$. This value of C_0 permits both tearing and surface preserving modes to exist simultaneously. Due to the presence of tearing mode, the initially straight magnetic field lines evolve and then form an island. However, unlike the only tearing mode case (for $C_0 = 0$), the island formed in this case is asymmetric (see Fig. 9). The asymmetry is also observed in the evolution of out-of-plane magnetic

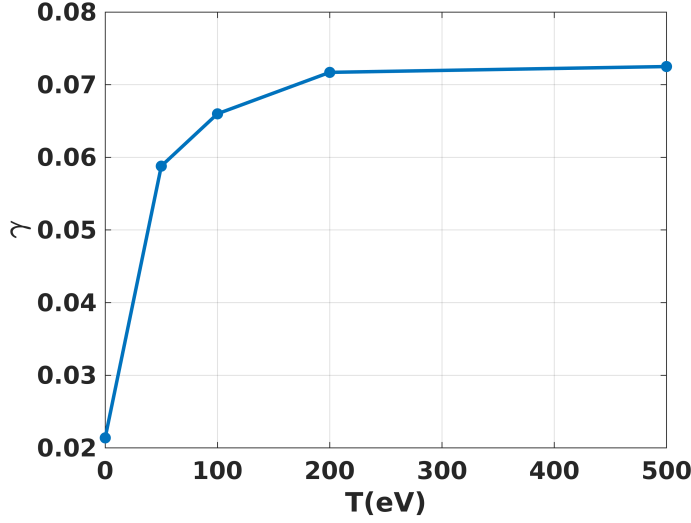


Figure 8. Variation in growth rate as a function of temperature (T) in eV, calculated from the perturbed energy evolution for the only surface preserving mode case ($C_0 = 0.06$).

field, the quadrupole formed is asymmetric.

Another interesting observation we made is that the island does not remain at its original location; it moves towards the left, the side with the weaker magnetic field. In Fig. 10, we see that initially the island forms at the null-line, denoted by a vertical line (at $x = -0.2661$), and it is asymmetric. As time progresses, the island shifts leftward. As seen in last subplot, the island has moved away from the vertical null-line. In contrast, in the case of only the tearing mode, a symmetric island forms at the null-line (at $x = 0.0$ in this case) and remains there, as shown in various subplots of Fig. 11. Shaded isocontours of equilibrium current show the formation of mushroom-like patterns. Two jet-like electron flows emerge from the neighboring X -points, which are essentially the outflows from two adjacent reconnection sites. These flows collide at the center of the O -point and then move perpendicularly to impact the closed magnetic surfaces on opposite sides, creating the mushroom-like structures. In the mixed modes case, the two electron flows encounter different strengths of the magnetic field on either side of the null-point. The stronger magnetic field experiences less bending due to higher magnetic tension. The collision of electron flows with magnetic surfaces of unequal strengths results in a net momentum toward the left. This net momentum causes the island and other structures to move in the negative x -direction. The unequal magnetic field strength on the two sides of the null-line is also the reason behind the formation of asymmetric structures. Some of these features have been reported in studies on asymmetric magnetic reconnection, which has recently garnered significant interest.

To understand the role of temperature, we conducted simulation runs for the following temperature values: $T = 5, 10, 20, 50, 100, 200, 500$ electron volts. Figure 12 depicts the change in growth rate with temperature for this case. Similar to the case

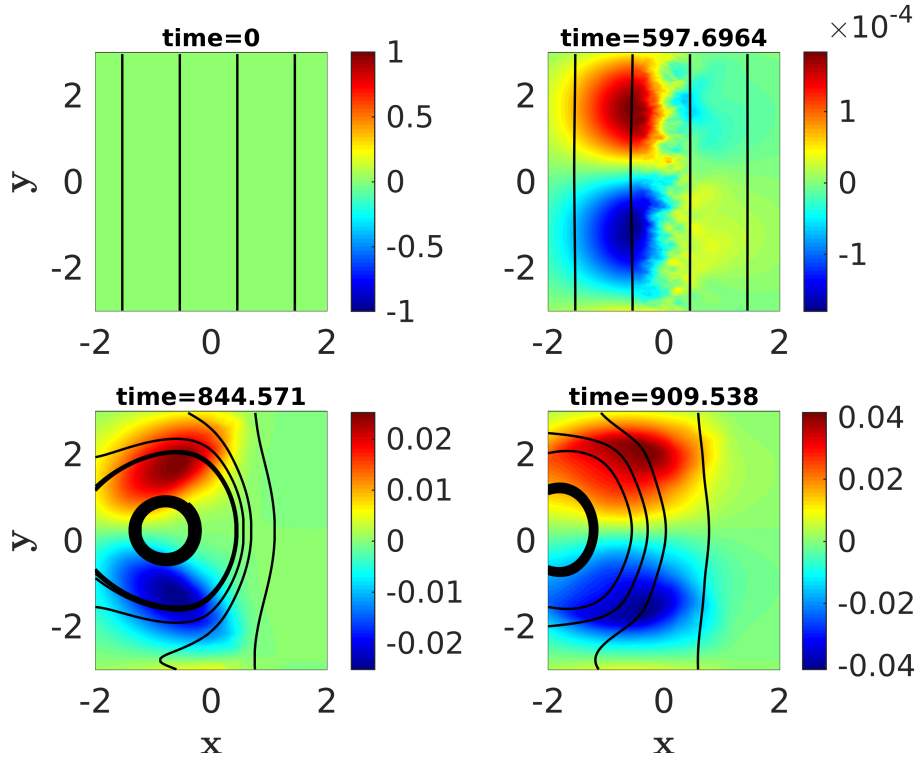


Figure 9. Shaded isocontours of out-of-plane magnetic field with superimposed streamlines (solid lines) over various times for mixed-modes case ($C_0 = 0.025$) and $T = 0$ eV case.

with only the tearing mode, the growth rate first increases with temperature and then starts decreasing. However, the peak of the curve has shifted to a lower temperature. Specifically, the peak growth rate occurs around 5 eV, compared to 10 eV in the only tearing mode case. The reason for this leftward shift of the peak is not certain at present. It could be due to asymmetry in the magnetic field on two sides of the null-line, the co-existence of the surface-preserving mode, and the effect of temperature on them. A more detailed study is underway to understand this effect.

Comparison with the Existing Studies:

Resistive MHD model can not explain the fast reconnection. Collisionless reconnection is one of the most promising models to explain the same. A vast literature is available on collisionless reconnection where hall term and inertia term become important. But most of these studies include the ion motion as well. Electron scale tearing mode is considered to be a prominent mechanism behind the fast reconnection. Studies that focus on the motion of only electrons by assuming the ions to be at rest, like our studies presented in this paper. We compare our results with the previous studies those have considered electrons motion only.

Electron scale tearing instability has been studied using Electron Magnetohydrodynamics (EMHD) model and Particle-In-Cell (PIC) simulations. Cai and Li [29], studied

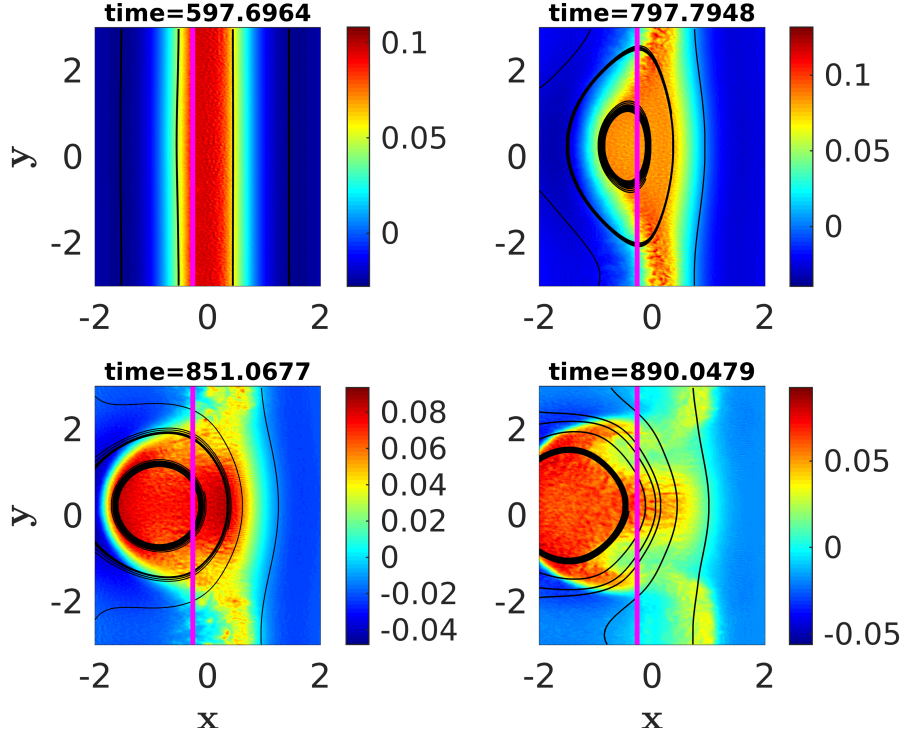


Figure 10. Shaded isocontours of the current J_z with superimposed streamlines (black lines) over various times for mixed-modes case ($C_0 = 0.025$) and $T = 0$ eV case.

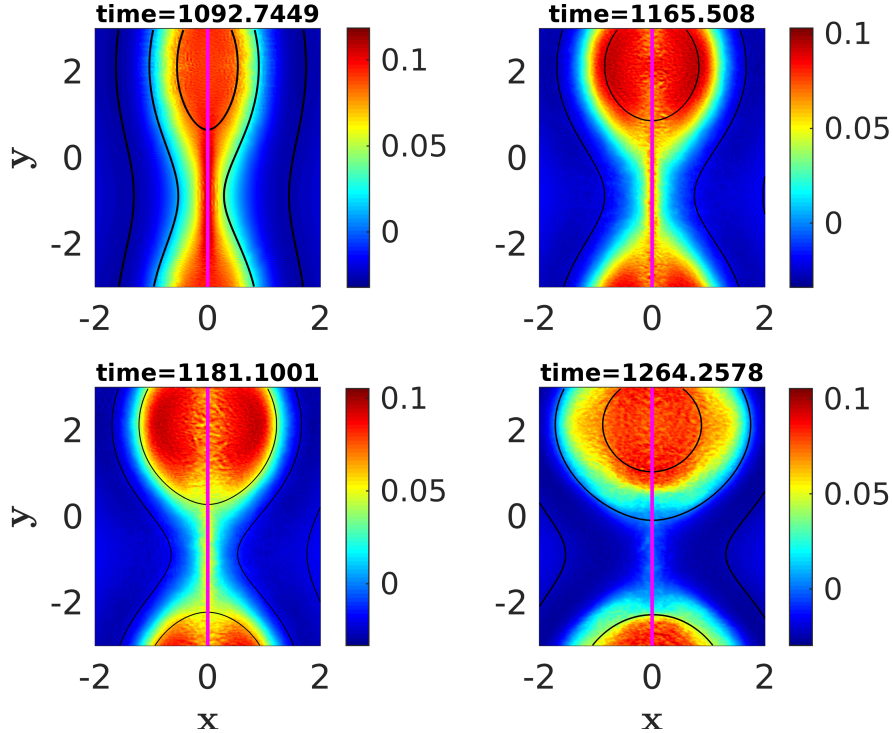


Figure 11. Shaded isocontours of the current J_z with superimposed streamlines (black lines) over various times for pure tearing mode case ($C_0 = 0$) and $T = 0$ eV case.

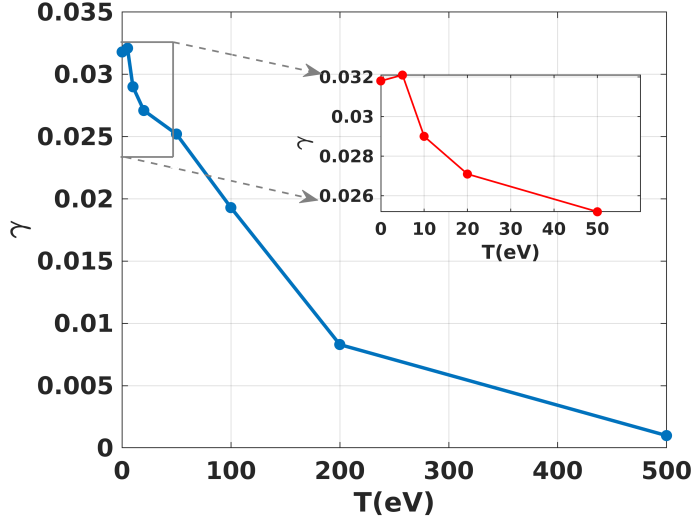


Figure 12. Variation in growth rate as a function of temperature (T) in eV, calculated from the perturbed energy evolution for the mixed-modes case ($C_0 = 0.025$). The inset presents a closer look at the growth rates for temperatures of 0, 5, 10, 20, and 50 eV.

the pressure gradient effects on tearing mode in the presence of guide magnetic field by including the electron pressure tensor, using EMHD model. Our numerical simulations are consistent with their analytical studies which show that when the electron thermal Larmor radius becomes sufficiently large, it can suppress the tearing mode instability. In one of their earlier works, Cai and Li [30], had included the compressible effects. However, our PIC simulations do not include the compressible effects and focus on the kinetic effects and specifically examine how temperature variations influence the tearing mode. Studies by Cai et al., are limited to linear regime only, while our simulations explore the nonlinear regime as well.

Jain & Büchner [20] conducted 3D linear studies focusing on tearing and non-tearing modes, examining the dependence of growth rate on the thickness of the electron current sheet, the strength of the guide field, and the wavenumber of the modes. Later, Jain et al. [21] performed 3D simulations to study these effects in the nonlinear regime. The key difference in our work is the inclusion of temperature effects, with no perturbations assumed along the equilibrium velocity current.

Guo et al. [31] analyzed the density and pressure gradient effects on the tearing mode in the context of 2D EMHD to study the electron diamagnetic drift and Biermann battery effects. In their later studies, Guo et al. [32] explores the tearing mode instability within electron-skin-depth-scale current sheets using EMHD model. The study conducts linear simulations of the tearing mode in both Harris sheet and force-free current sheet configurations, revealing that resistive diffusion is negligible at this scale. Additionally, the study examines the impact of a strong magnetic guide field and shear flow, finding that shear flow can suppress the tearing mode in a force-free equilibrium state. Our research, on the other hand, does not consider density and pressure gradients or shear

flow, but rather focuses on the interplay between electron temperature and the guide field.

The contour plots for magnetic field, current and other fields observed in our PIC simulations exhibit the same behavior as observed by Sarto et al. [33] during the fully nonlinear phase of the EMHD reconnection. We have also observed the secondary electron Kelvin – Helmholtz instability of the current jets originating from two nearby X points colliding at the O point. However, in the case of mixed mode, we observe that the collision of the two jets results in the net momentum and make the island and other structure move from the position they initially form. No such phenomena was observed in the case of only surface-preserving mode case.

Betar et al. [34] conducted a numerical study on the linear dynamics of tearing modes within a slab incompressible EMHD framework, accounting for the influence of more than one non-ideal parameters such as electron inertia, resistivity and electron viscosity. Their findings emphasize the need for future research to incorporate kinetic effects and investigate EMHD tearing mode regimes, such as “electron-only” reconnection.

Zhao [35] incorporated the temperature in the warm EMHD model and derived the dispersion relation and investigated the electromagnetic properties of obliquely propagating whistler waves. As a future work, the warm EMHD model discussed by Zhao can be used to study linear growth rate and eigen structure of tearing and surface preserving modes change at low to moderate temperature (at high temperature, the EMHD model would break). The work on the same is underway.

4. Summary and Future Scope

In this study, we conducted two-dimensional PIC simulations using the OSIRIS framework to investigate the kinetic effects on tearing and surface-preserving instabilities in electron current layers, which are relevant to various space, astrophysical, and laboratory plasma environments. We started by simulating the conventional tearing instability to validate our simulation setup. After validation, we explored the kinetic effects on the tearing mode by varying the electron temperature. Our results show that the growth rate of the tearing instability initially increased with temperature, peaking around 10 eV, before declining due to the increased electron Larmor radius and consequent diffusion of magnetic fields. To support our argument, we introduced a uniform guide field, which exhibited a stabilizing effect on the tearing mode, resulting in a shift of the peak growth rate to higher temperatures.

To study the surface-preserving instability, we added a uniform magnetic field $C_0 = 0.06$ along the equilibrium magnetic field direction, which inhibits the tearing mode in the system. To analyze the effect of temperature on the growth rate of this mode, we ran simulations at various temperatures. The growth rate versus temperature plot shows a consistent rise, which can be attributed to the increased electron flow velocity at higher temperatures. This rise favors the instability, as it is driven by

perturbations in the flow.

Finally, we also investigated the case when both the tearing and surface-preserving modes exist simultaneously in the system. Simulation runs in this scenario show that the structures (island and quadrupole) formed are asymmetric. Moreover, these structures do not remain stationary but move towards the weaker magnetic field side around the null-line. This behavior aligns with findings from studies on asymmetric magnetic reconnection. The growth rate's temperature dependence follows a pattern similar to the pure tearing mode case, initially increasing with temperature but peaking at lower temperature value. The causes of this shift are currently being studied, considering magnetic field asymmetries and the interplay between tearing and surface-preserving modes under varying temperatures.

Future Directions:

- In our studies, we have chosen the tanh - sech profile for the equilibrium magnetic field. While this allows us to use periodic boundary conditions, the profile naturally ceases at the boundaries. Conducting studies on larger systems (using profiles with a larger extent) with appropriate boundary conditions would provide a natural comparison.
- In our studies, we have chosen $\epsilon = 1$, which is normalized by the electron skin depth. A parametric study by choosing $\epsilon > 1$ and $\epsilon < 1$ needs to be carried out to understand the behavior of the two modes in these different regimes, along with the role of temperature on their behavior.
- In mixed mode cases, the magnetic field profile is asymmetric around the null line. To distinguish the effects of this asymmetry on the tearing mode and its interaction with the surface-preserving mode, a dedicated study using appropriate profiles is needed.
- Linear stability analysis using a warm EMHD (Electromagnetic Magnetohydrodynamics) model is currently underway and is essential for understanding the eigenmode structure under varying temperature conditions. This analysis will provide insights into how temperature influences the structure and stability of the modes.

References

- [1] Birn J and Priest E R 2007 *Reconnection of magnetic fields: magnetohydrodynamics and collisionless theory and observations* (Cambridge University Press)
- [2] Biskamp D 1996 *Astrophysics and Space Science* **242** 165–207
- [3] Yamada M, Kulsrud R and Ji H 2010 *Reviews of modern physics* **82** 603
- [4] Taylor J B 1986 *Reviews of Modern Physics* **58** 741
- [5] Yamada M 1999 *Journal of Geophysical Research: Space Physics* **104** 14529–14541
- [6] Stenzel R, Griskey M, Urrutia J and Strohmaier K 2003 *Physics of Plasmas* **10** 2780–2793
- [7] Stenzel R, Griskey M, Urrutia J and Strohmaier K 2003 *Physics of Plasmas* **10** 2810–2818
- [8] Bose S, Fox W, Ji H, Yoo J, Goodman A, Alt A and Yamada M 2024 *Physical Review Letters* **132** 205102

- [9] Sweet P A 1958 *Electromagnetic Phenomena in Cosmical Physics* 123–134
- [10] Parker E N 1957 *Journal of Geophysical Research* **62**(4) 509–520
- [11] Petschek H E 1964 *NASA Special Publication* **50** 425
- [12] Bulanov S, Pegoraro F and Sakharov A 1992 *Physics of Fluids B: Plasma Physics* **4** 2499–2508
- [13] Gaur G and Kaw P K 2016 *Physics of Plasmas* **23**
- [14] Shay M A, Drake J F, Denton R E and Biskamp D 1998 *Journal of Geophysical Research: Space Physics* **103** 9165–9176
- [15] Drake J, Shay M and Swisdak M 2008 *Physics of Plasmas* **15**
- [16] Matthews A P 1994 *Journal of Computational Physics* **112** 102–116
- [17] Daughton W, Roytershteyn V, Albright B, Karimabadi H, Yin L and Bowers K J 2009 *Physical review letters* **103** 065004
- [18] Horiuchi R and Sato T 1999 *Physics of Plasmas* **6** 4565–4574
- [19] Lukin V 2009 *Physics of Plasmas* **16**
- [20] Jain N and Büchner J 2015 *Journal of Plasma Physics* **81** 905810606
- [21] Jain N, Büchner J and Muñoz P A 2017 *Physics of Plasmas* **24**
- [22] Dawson J M 1983 *Reviews of modern physics* **55** 403
- [23] Hockney R W and Eastwood J W 2021 *Computer simulation using particles* (crc Press)
- [24] Fonseca R, Silva L, Tsung F, Decyk V, Lu W, Ren C, Mori W, Deng S, Lee S, Katsouleas T *et al.* 2002 *Lecture Notes in Computer Science* **2331** 342–351
- [25] Fonseca R A, Vieira J, Fiúza F, Davidson A, Tsung F S, Mori W B and Silva L O 2013 *Plasma Physics and Controlled Fusion* **55** 124011
- [26] Kemp A, Fiúza F, Debayle A, Johzaki T, Mori W, Patel P, Sentoku Y and Silva L 2014 *Nuclear Fusion* **54** 054002
- [27] Silva L O, Fonseca R, Tonge J, Dawson J, Mori W and Medvedev M 2003 *The Astrophysical Journal* **596** L121
- [28] Fonseca R, Dalichaouch T, Davidson A, Cruz F, Del Gaudio F, Inchingolo G, Helm A, Lee R, Li F, May J *et al.* 2018 Osiris 4.0: A state of the art framework for kinetic plasma simulations *APS Division of Plasma Physics Meeting Abstracts* vol 2018 pp PP11–023
- [29] Cai H and Li D 2009 *Physics of Plasmas* **16**
- [30] Cai H and Li D 2008 *Physics of Plasmas* **15**
- [31] Guo W, Liu D, Wang X and Wang J 2020 *AIP Advances* **10**
- [32] Guo W, Wang J and Liu D 2021 *AIP Advances* **11**
- [33] Del Sarto D, Califano F and Pegoraro F 2005 *Physics of plasmas* **12**
- [34] Betar H, Del Sarto D, Ghizzo A, Brochard F and Zarzoso D 2024 *Physics of Plasmas* **31**
- [35] Zhao J 2017 *The Astrophysical Journal* **850** 13